Chalcogenide Letters Vol. 18, No. 10, October 2021, p. 557 - 564

Tribological properties of electrospark depositing Ni-WS_2 self-lubricating coating

M. Yue[a], W. Zhao[b], S. Wang[a,c*], J. Li[b], C. Zhu[d], H. Jin[a,d], C. Guo[a]
[a]*School of Equipment Engineering, Shenyang Ligong University, Shenyang 110159, China*
[b]*Liaoshen lndusteries Croup Co. Ltd, Shenyang 110045, China*
[c]*State Key Laboratory of Explosion Science and Technology, Beijing Institute of Technology, Beijing 100081, China*
[d]*Chongqing Chang'an Industry (Group) Co. Ltd, Chongqing 401120, China*

A Ni-WS_2 sintered electrode was used to prepare a coating on a CrNi3MoVA steel substrate by employing electrospark deposition technique. The nanomechanical and tribological properties of the coating were tested by using nanoindenter and tribometer, and the morphologies, composition and phase structure were obtained by utilizing scanning electron microscopy (SEM), energy dispersive X-ray spectrum (EDS) and X-ray diffraction(XRD). The results showed that the coating is even-distributed with nanostalline α-W strengthening phase dopants, and it has a strong metallurgical bonding with the substrate. The coating is composed of WS_2, γ-Ni, α-W and Ni_3S_2 phases, and it exhibits outstanding tribological properties for its friction coefficient reduced about 79% and wear rate reduced about 96% in contrast to the CrNi3MoVA steel.

(Received July 20, 2021; Accepted October 2, 2021)

Keywords: Self-lubricating coating, Electrospark deposition, Ni-WS_2, Tribological properties

1. Introduction

Self-lubricating composites with solid lubricant can form a continuous transfer film to realize the function of friction reduction and wear resistance increase in the environment of friction and wear, and in contrast to the traditional methods of adding liquid or semi-solid grease at the friction interface, they are more adaptive for meeting the requirement under the serve condition of vacuum, high-pressure, high-temperature, high-speed, radiation, etc. Therefore there has been much intense research about the self-lubricating composites with solid lubricant for many decades. Transition metal dichalcogenides, especially MoS_2 and WS_2, as solid lubricant, have been widely investigated in the tribological field, and their outstanding tribological properties are mainly attributed to the layered structure, in which a sheet of metal (Mo or W) is sandwiched between two hexagonally packed sulfur layers. Within the layers bonding is covalent, while the sandwich is held together through weak Van der Waal's bonding. Hence, the basal planes easily slide over one another under a shearing load, resulting in a low friction coefficient at the rubbing counterface [1].

As wear always takes place on a key component surface, self-lubricating coatings with transition metal dichalcogenides are generally prepared to improve the surface tribological properties [2-3]. Although transition metal dichalcogenides have excellent tribological properties in ultrahigh vacuum or in inert gas environment, their friction coefficient and wear rate will increase rapidly in humid air due to the reaction of dangling or unsaturated bonds on the edge of basal planes with moisture and oxygen in the surrounding environment, leading to eventual coating premature failure. To solve these problems, there have been many investigations about doping metal or oxide in transition metal dichalcogenides to improve their tribological properties in humid air. The dopants, such as Ti [4-5], Ni [2, 6-9], Cr [10], Sb_2O_3 [1, 11], etc., can increase coating density, hardness and oxidation resistance.

Eletrodepostion, electroless plating, thermal spraying and laser cladding [12] are widely employed to prepare self-lubricating coatings with transition metal dichalcogenides. However, the

*Corresponding author: zbgc2021@aliyun.com
https://doi.org/10.15251/CL.2021.1810.557

bonding between coating and substrate by the first three techniques is weak while the laser cladding may induce serious substrate deterioration, so it is desirable to develop a new technique to avoid the above disadvantages. Electrospark deposition (ESD) is a surface technique to prepare metallurgical bonded coatings with outstanding properties on metallic substrate materials, and it eliminates distortion or metallurgical changes in substrate due to low heat input. Besides, it is also a simple, cost-effective, easily automated and environment-friendly technique applied in many industrial fields [13-14]. Recently C. Guo, et al. [2] studied the performance of friction and wear of the Ni-MoS_2 self-lubricating coatings prepared by ESD, showing that the coating exhibits excellent tribological properties due to the synergistic effect of MoS_2 and MoO_2 in the coating, which indicates that ESD technique has a promising prospect for preparing self-lubricating coatings with transition metal dichalcogenides. According to previous investigations, WS_2 has better oxidation resistance and thermal stability than MoS_2, and its tribological properties have been investigated less extensively in contrast to MoS_2. To the best knowledge of the authors, there is still no relevant research report about a Ni-WS_2 self-lubricating coating prepared by ESD technique. Hence, in this work, the tribological properties of an ESD Ni-WS_2 self-lubricating coating on a CrNi3MoVA steel substrate will be investigated.

2. Materials and methods

The CrNi3MoVA steel was selected as the substrate material and its chemical composition is shown in table 1. A bar of CrNi3MoVA steel was processed into rectangle-shape specimens with a size of 20 mm×10 mm×3 mm by wire electrical discharge machining. The nickel matrix self-lubricating composite (hereafter abbreviated as Ni-WS_2 composite) was prepared by spark plasma sintering (SPS) using a mixture of argon-atomized nickle powder (50 wt%) and WS_2 powder (50 wt%). The mean particle size of Ni was about 50 μm, and that of WS_2 about 10 μm, and their purity was more than 99.9%. The mixed raw powders were blended by high energy ball milling manner for 8 h before filled in a graphite die, and then sintered in a KCE-FCT HP D 250-C furnace (made in Germany) under the vacuum of 0.1 Pa. The Ni-WS_2 composite was heated from room temperature (RT) to 1373 K at a heating rate of 50 K/min, and then sintered at 1323 K under the pressure of 40 MPa for 10 min. Next it cooled to 923 K at a heating rate of 30 K/min in furnace. After that, it naturally cooled to room temperature in air. The bar of sintered Ni-WS_2 composite was processed into a cylinder-shape electrode with a size of Φ4 mm×50 mm and rectangle-shape specimens with a size of 20 mm×10 mm×3 mm respectively by wire electrical discharge machining. The specimens (CrNi3MoVA steel and Ni-WS_2 composite) and electrode were ground by using SiC abrasive paper up to an 800 grit finish, and then ultrasonically cleaned in ethanol and acetone mixture. The Ni-WS_2 self-lubricating coating (hereafter abbreviated as Ni-WS_2 coating) was prepared by using DJ-2000 type adjustable power metal surface repairing machine, and the optimized deposition parameters through preliminary tests set as outlined in Table 2.

Table 1. Chemical composition of CrNi3MoVA steel [2].

C	Mn	Si	Cr	Ni	Mo	V	S	P
0.40	0.41	0.25	1.28	3.14	0.37	0.20	0.001	0.012

Table 2. Processing parameters of ESD Ni-WS_2 coating.

Power/W	Ar gas flow/L·min^{-1}	Electrode rotating rate/r·min^{-1}	Deposition time unit area/min·cm^{-1}
1000	15	3000	2.0

The hardness and elasticity modulus of the CrNi3MoVA steel, Ni-WS_2 composite and Ni-WS_2 coating were tested by employing nano-indentaion G200 with Berkovich indenter and calculated by Oliver-pharr model through loading curves, and the tested values are the average values of ten parallel tested points on the surface of the specimens. The tribological properties were tested by using an HSR-2M reciprocating tribometer. The material of grinding head is a quenched GCr15 steel ball with a diameter of 6 mm, the reciprocating distance 5 mm, the reciprocating speed 0.1 m per second, the load 2 N and the total rubbing time 5 min. The wear rate (W, $mm^3\ N^{-1}\ m^{-1}$) of the specimens was calculated through the volume of wear trace using the following equation [15]:

$$W = \frac{d^2 \times h\{2 \times \arcsin\left(\frac{L}{d}\right) - \sin[\,2 \times \arcsin\left(\frac{L}{d}\right)]\}}{8 \times F \times v \times t}$$

where d is the diameter of grinding ball (d=6 mm), t is the sliding time (h=300 s), h and L are the length and width of wear track, respectively.

Original and worn morphologies were characterized by scanning electron microscopy (SEM, TESCAN MAIA3, Czech Republic), while the energy-dispersive spectrometer (EDS, X-Max, United Kingdom) was utilized to analyze the chemical composition of a selected-area. The phase constitutions of the Ni-WS_2 composite and coating were identified by X-ray diffraction (XRD, X' Pert PRO, Holland).

3. Results and discussion

3.1. Ni-WS_2 coating microstructure

Fig. 1 shows the surface morphology (a) and EDS results of area A (b) of the Ni-WS_2 coating. The surface morphology of the Ni-WS_2 coating displays a solidification feature of liquid splashing and overlapping by the plasma jet in argon at high speed. The EDS results of area A of the Ni-WS_2 coating indicate that the coating surface has almost the same composition as the composite electrode, and only a very small fraction of Fe diffuses from the substrate to the coating surface.

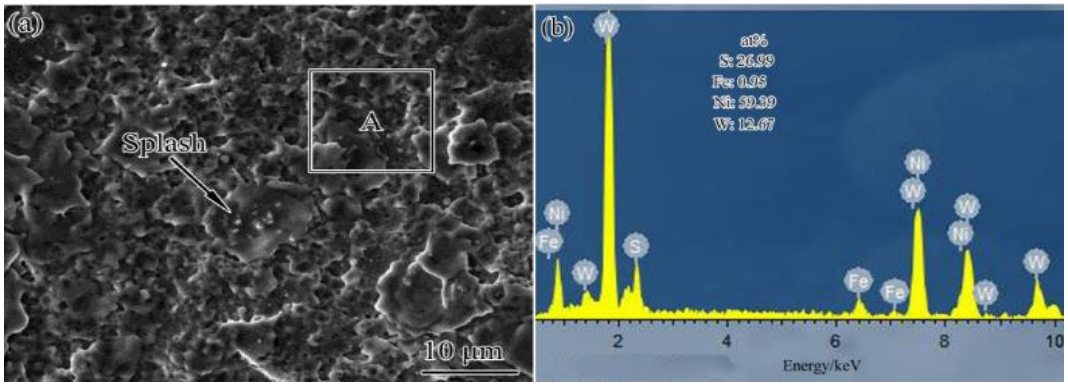

Fig. 1. Surface morphology (a) and EDS results of area A (b) of Ni-WS_2 coating

Fig. 2 shows the cross-section (backscattered electron) morphology (a), EDS line scanning (b), and EDS results of point B (c) of the Ni-WS_2 coating. As shown in Fig. 2a, the thickness of the Ni-WS_2 coating is about 8 μm and its dense microstructure is even-distributed with many white dots with a size of submicron and even nanometer scale. The EDS line scanning (Fig. 2b) of the Ni-WS_2 coating displays that there is a gradual transition region of Ni and Fe, indicating that the interdiffusion takes place between the coating and the substrate to form a strong metallurgical bonding. The EDS results of point B (marked as an arrow in Fig. 2c) of the Ni-WS_2 coating show

that the white dot is a W-rich phase.

Fig. 3 shows the XRD patterns of the Ni-WS_2 composite and its ESD coating. The Ni-WS_2 compostie and its ESD coating are both composed of WS_2, γ-Ni, α-W and Ni_3S_2 phases. However, the peaks of WS_2 and γ-Ni in the Ni-WS_2 coating are stronger than those in the Ni-WS_2 composite while the peaks of α-W and Ni_3S_2 in the Ni-WS_2 coating are weaker compared with those in the Ni-WS_2 composite, indicating that the ESD process could facilitate WS_2 formation. As WS_2 has a low decomposition temperature (783 K), it will decompose even if it is well encapsulated by high-energy milling of Ni particles [9]. According to the Gibbs free energy change of WS_2 and Ni_3S_2 at various temperatures (Fig. 4), when the temperature is over 1000 K, the Gibbs free energy of Ni_3S_2 is more negative than that of WS_2, so the following reaction could be favored in light of thermodynamics:

$$WS_2+3Ni=Ni_3S_2+W$$

Thus the sinered Ni-WS_2 composite contains a mass of α-W and Ni_3S_2 phase. In ESD process, heat is generated in 1 % of one pulse cycle, and then transferred in the rest of 99 % of one pulse cycle due to a short pulse duration and a high frequency, so the cooling speed may reach in the range of 10^5-10^6 K/s [2, 13-14], and such fast solidification can be utilized to prepared coatings containing nano-sized grains. Combining with the EDS results of point B (Fig. 2c), the white W-rich phase with nanometer scale could be α-W, and nanocrystalline could increase the activity of W. Moreover, the plasma arc generated by the current pulse can reach 5000-25000 K, and the α-W in the Ni-WS_2 electrode will transform from solid phase to liquid one, which could also increase the activity of W. Therefore the above reaction could be favored in the opposite direction in EDS process based on kinetics.

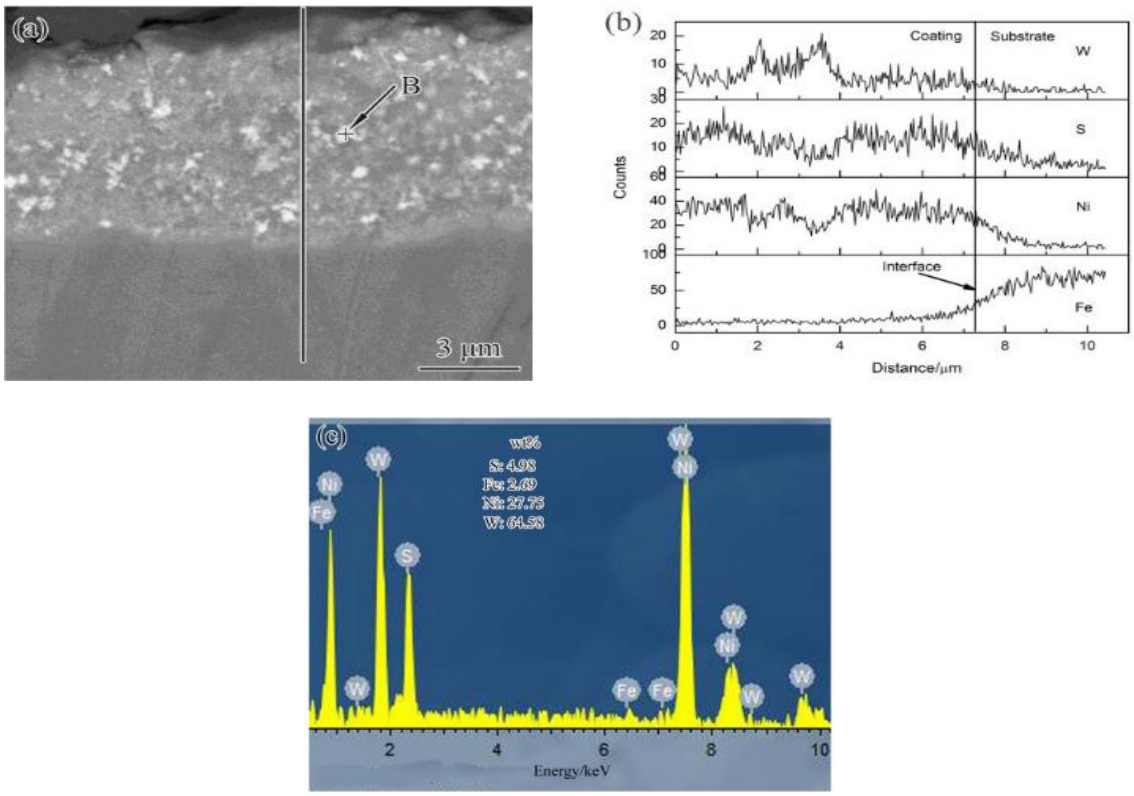

Fig. 2. Cross-section BSE (backscattered electron) morphology (a), EDS line scanning (b), and EDS results of point B (c) of Ni-WS_2 coating.

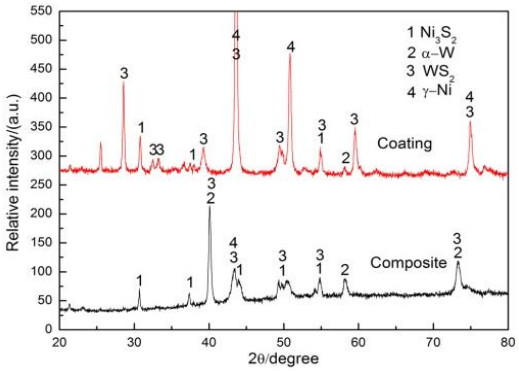

Fig. 3. XRD patterns of Ni-WS_2 composite and its ESD coating.

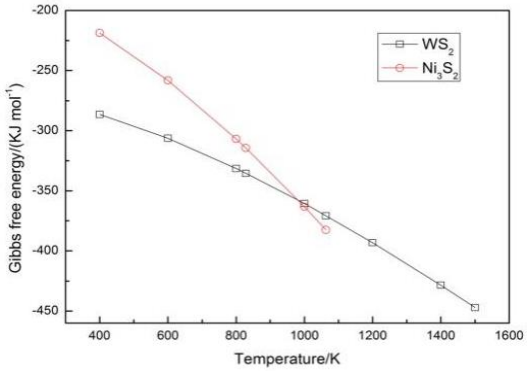

Fig. 4. Gibbs free energy change of WS_2 and Ni_3S_2 at various temperatures

3.2. Nano-mechanical properties of CrNi3MoVA steel, Ni-WS_2 composite and its ESD coating

Table 3 shows the nano-mechanical properties of the CrNi3MoVA steel, Ni-WS_2 composite and its ESD coating. Deepthi B. et al. [10] reported that the WS_2 coating exhibited a hardness of 1.5 GPa and elastic modulus of 48 GPa, and compared with their results, the hardness of the Ni-WS_2 coating increases 2.58 times in this work. The increased hardness of the Ni-WS_2 coating may be attributed to solution hardening, refined crystalline strengthening and dense microstructure prepared by ESD technique. Moreover, the hardness of the Ni-WS_2 coating increases about 8.7% than that of the Ni-WS_2 composite due to the different proportion of phase constitution. Meanwhile, H/E ratio, associated with increased elasticity, is used to determine elastic behavior limit in a surface contact [2, 13], and a specimen with higher H/E ratio usually means a higher critical load for elastic-plastic transition. The H/E ratio of the Ni-WS_2 coating increases about 78% than that of the CrNi3MoVA steel, suggesting that the Ni-WS_2 coating have better wear resistance than the CrNi3MoVA steel.

Table 3. Nano-mechanical properties of CrNi3MoVA steel, Ni-WS_2 composite and its ESD coating.

Samples	H (GPa)	E (GPa)	H/E
CrNi3MoVA steel	4.62	261.8	0.018
Ni-WS_2 composite	4.94	152.5	0.032
Ni-WS_2 coating	5.37	149.8	0.036

3.3. Tribological properties of CrNi3MoVA steel, Ni-WS_2 composite and its ESD coating

Fig. 5 shows the worn morphologies of low magnification (a) and zone C magnification (b) of the CrNi3MoVA steel, low magnification (c) and zone D magnification (d) of the Ni-WS_2 composite, and low magnification (e) and zone E magnification (f) of the Ni-WS_2 coating. As shown in Fig. 5a, 5c and 5e, the width of wear tracks of the Ni-WS_2 coating is only 72 μm, far less than that of the CrNi3MoVA steel (511 μm), and the Ni-WS_2 composite (339 μm). As shown in Fig. 5b magnified from zone C, there is a deep ploughing groove on the worn surface of the CrNi3MoVA steel and two big strips of ploughed adhesion worn debris beside the groove, indicating that the severe plastic flow occurred on the rubbing contact surface of the CrNi3MoVA steel. Therefore the main wear mechanism of the CrNi3MoVA steel belongs to severe adhesive wear. As shown in Fig. 5d magnified from zone D, there are obvious cracks and large area of spalling region on the worn surface of the Ni-WS_2 composite, so the main wear mechanism of the Ni-WS_2 composite can be characterized as peeling wear. As shown in Fig. 5f magnified from zone E, the worn surface of the Ni-WS_2 coating is distributed with several micro-cracks that are difficult to identify even at high magnification, and it is much smoother than the surface of the as-deposited coating. Thus the main wear mechanism of the Ni-WS_2 coating is slight adhesive wear.

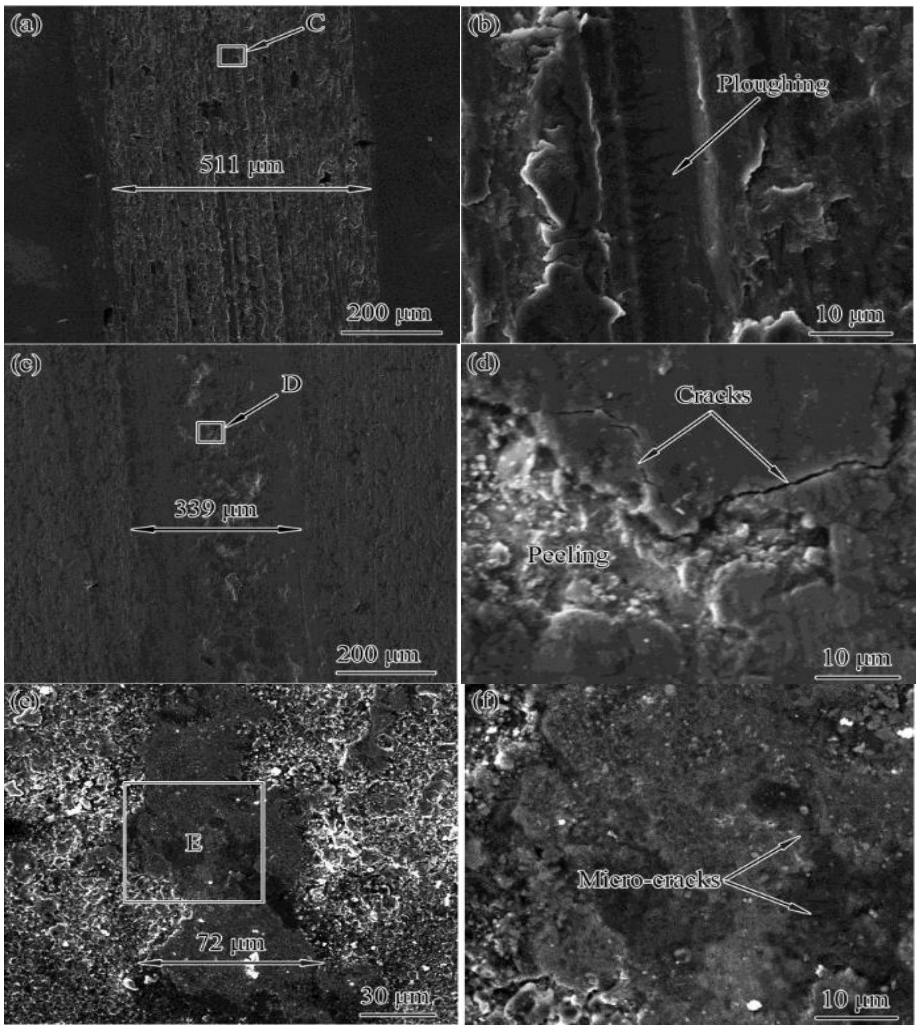

Fig. 5. Worn morphologies of low magnification (a) and zone C magnification (b) of CrNi3MoVA steel, low magnification (c) and zone D magnification (d) of Ni-WS_2 composite, and low magnification (e) and zone E magnification (f) of Ni-WS_2 coating

Fig. 6 shows the friction coefficient (a) and wear rate (b) of the CrNi3MoVA steel, Ni-WS_2 composite and its ESD coating. As shown in Fig. 6a, the steady friction coefficient of the CrNi3MoVA steel is 0.68-0.73 whilst that of the Ni-WS_2 coating only 0.14-0.16. The friction coefficient of the Ni-WS_2 composite is in between, and can't attain a steady state because of fluctuating greatly. The friction coefficient of the Ni-WS_2 coating reduced about 79% than that of the CrNi3MoVA steel, suggesting that the Ni-WS_2 coating has a noticeable antifriciton effect on the CrNi3MoVA steel. Meanwhile, as shown in Fig. 6b, the wear rate of the Ni-WS_2 coating increased about 96%, 87% than that of the CrNi3MoVA steel, and Ni-WS_2 composite, respectively.

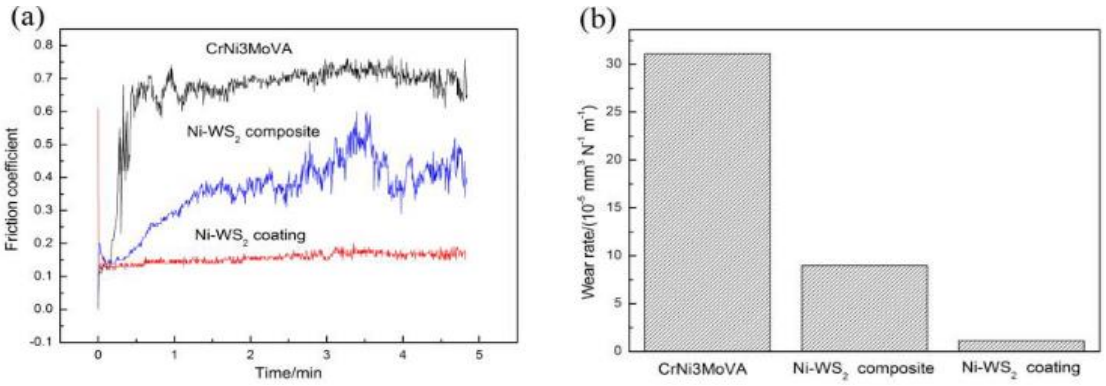

Fig. 6. Friction coefficient (a) and wear rate (b) of CrNi3MoVA steel, Ni-WS_2 composite and its ESD coating.

It is believed that the transfer film of WS_2 in the rubbing contact surface is the main factor that influence the tribological properties of the Ni-WS_2 coating, and the dopants of γ-Ni, α-W and Ni_3S_2 surround around the WS_2 to increase its oxidation resistance in humid air for a long period. Furthermore, the ESD process facilitates the WS_2 formation by using a sinered Ni-WS_2 electrode. Moreover, the dense microstructure, refined grains, and α-W nanocrystalline strengthening phase produced by ESD technique increase the hardness and H/E ratio of the Ni-WS_2 coating, which all favor the increase of the wear resistance. In addition, the ESD Ni-WS_2 coating has a strong metallurgical bonding with the substrate, which can also improve the tribological properties.

4. Conclusions

The dense Ni-WS_2 coating is even-distributed with nanocrystalline α-W strengthening phase and has a strong metallurgical bonding with the substrate. The Ni-WS_2 coating consists of WS_2, γ-Ni, α-W and Ni_3S_2, and ESD process facilitates the WS_2 formation by using a sinered Ni-WS_2 electrode. The friction coefficient of the Ni-WS_2 coating reduced about 79%, and the wear resistance increased about 96% than that of the CrNi3MoVA steel.

Acknowledgments

The authors are grateful for the financial support of the National Science Foundation of Liaoning Province of China (No.20180550353, 2019-ZD-0264), and the Basic Research Project of Education Department of Liaoning Province of China (No.LG202006), and the Supporting Project of Middle-young Aged Innovative Talents of Science and Technology of Shenyang City (RC190292), and the Supporting Project of Innovative Talents of Colleges and Universities of Liaoning Province (LR2019059), and the Research Innovation Team Building Program of Shenyang Ligong University.

References

[1] T. W. Scharf, P. G. Kotula, S. V. Prasad, Acta Materialia **58**, 4100 (2010).
[2] C. Guo, F. Kong, S. Zhao, X. Yan, J. Yang, J. Zhang, Chalcogenide Letters **16**(7), 309 (2019).
[3] Y. Liao, B. Zhang, M. Chen, M. Feng, J. Wang, S. Zhu, F. Wang, Corrosion Science **167**, 108526 (2020).
[4] D. G. Teer, Wear **251**, 1068 (2001).
[5] T. W. Scharf, A. Rajendran, R. Banerjee, F. Sequeda, Thin Solid Films **517**, 5666 (2009).
[6] J. Xu, W. Liu, M. Zhong, Surface & Coatings Technology **200**, 4227 (2006).
[7] T. Cao, S. Lei, M. Zhang, Surface and Coatings Technology **270**, 24 (2015).
[8] S. Xu, X. Gao, M. Hu, J. Sun, D. Jiang, F. Zhou, W. Liu, L. Weng, Applied Surface Science **288**, 15 (2014).
[9] A. Wang, X. Zhang, X. Zhang, X. Qiao, H. Xu, C. Xie, Materials Science & Engineering A **475**, 372 (2008).
[10] B. Deepthi, H. C. Barshilia, K.S. Rajam, M. S. Konchady, D. M. Pai, J. Sankar, A. V. Kvit, Surface & Coatings Technology **205**, 1937 (2010).
[11] J. J. Hu, J. E. Bultman, J. S. Zabinski, Tribology letters **21**, 169 (2006).
[12] J. Wang, S. Jiang, X. Zhu, Materials Reports **33**, 2868 (2019).
[13] C. Guo, Z. Zhao, F. Lu, B. Zhao, S. Zhao, J. Zhang, Digest Journal of Nanomaterials and Biostructures **13**(4), 931 (2018).
[14] C. Guo, T. Liang, F. Lu, B. Zhao, Z. Liang, S. Zhao, J. Zhang, Materials and Technology **53**(3), 389 (2019).
[15] Q. Wang, M. Chen, Z. Shan, C. Sui, L. Zhan, S. Zhu, F. Wang, Journal of Materials Science & Technology **33**, 1416 (2017).